

A Multiphysics Simulation Approach for Photonic Devices Integrating Phase Change Materials

Amin Shafiee[†], Benoit Charbonnier*, Sudeep Pasricha[†], and Mahdi Nikdast[†]

[†]Department of Electrical and Computer Engineering, Colorado State University, Fort Collins, CO, USA

*Université Grenoble Alpes, CEA, LETI, F38000, Grenoble, France

Abstract—This work presents a three-dimensional electromagnetic and heat-transfer multiphysics simulation approach for the design and optimization of photonic devices that integrate phase change materials (PCMs) for emerging photonic computing systems. Leveraging the multiphysics simulation, a PCM-based compact and low-loss phase shifter is designed with 24 μs latency for π phase shift and a maximum insertion loss of 0.3 dB/ π when the PCM is in the crystalline state.

I. INTRODUCTION

Silicon photonic devices have a wide range of applications from sensing to high-speed optical communication and computation. More recently, such devices have been integrated with phase change materials (PCMs) for improving reconfigurability and energy efficiency [1], [2] in emerging photonic computing (e.g., in-memory photonic computing [1]) and optical memory systems. However, exact simulation of PCM-based photonic devices is challenging due to the need for combining molecular-level (nucleation and growth), material-level (optical and electrical properties), and device-level (electromagnetic and optoelectronic) simulations [3]. To address this, some prior work has shown that the performance of PCM-based photonic devices can be estimated using multiphysics simulations [4]. In this paper, we present a comprehensive three-dimensional multiphysics simulation approach for PCM-based photonic devices, to design and optimize PCM-based photonic devices for emerging photonic computing and optical memory systems. The proposed simulation approach includes both thermal and opto-electrical simulations and their interplay using commercial tools, and help designers better understand what simulations are required to explore and optimize PCM-based photonic devices. As a case study and leveraging the proposed simulation approach, we present the design and optimization of a PCM-based silicon photonic phase modulator.

II. MODELLING OF PCM-BASED PHOTONIC DEVICES

The phase state of a PCM changes upon exposure to an external heat source, leading to different optical and electrical properties [1]. PCMs can be in amorphous, crystalline, or even an intermediate state where the material is partially crystallized [2]. When heated, depending on the temperature distribution, the phase state of PCMs can be estimated. The portion of the material with a temperature below the melting point and higher than the crystallization temperature can be considered to have a crystalline state. As the temperature of the material increases and reaches the melting temperature, the material

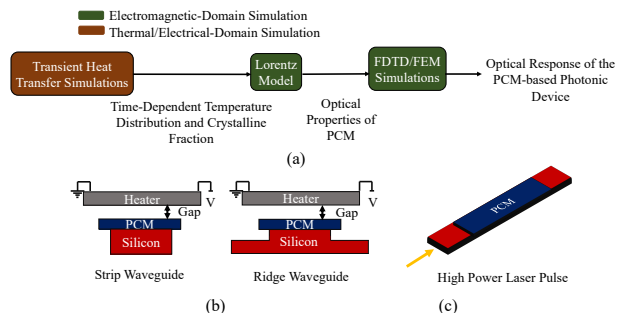


Fig. 1. (a) Multiphysics simulation steps for PCM-based photonic devices. PCM's phase state can be controlled using (b) a microheater and (c) a high-power laser pulse.

will be melted and quenched, and hence can be considered to be in the amorphous state. The time-dependent temperature distribution of PCMs can be analyzed by solving transient unsteady-state heat-transfer equations in the PCM volume [1], [5], as shown in Fig. 1(a). The required heat to trigger the phase transition in PCMs can be provided by joule heating using a microheater, or optically by using high-power laser pulses, as shown in Figs. 1(b) and 1(c), respectively.

Given the time-dependent temperature distribution in a PCM, the crystalline fraction, which determines the portion of the material with crystalline state, can be estimated [3]. By using the crystalline fraction (X_f) in the Lorentz model [1], [3], we can estimate optical properties of the PCM in any state, as defined below:

$$\frac{\varepsilon_{eff}(\lambda) - 1}{\varepsilon_{eff}(\lambda) + 2} = (X_f) \frac{\varepsilon_c(\lambda) - 1}{\varepsilon_c(\lambda) + 2} + (1 - X_f) \frac{\varepsilon_a(\lambda) - 1}{\varepsilon_a(\lambda) + 2}. \quad (1)$$

Here, X_f takes a number between 0 and 1, where $X_f = 0$ is used for fully amorphous state and $X_f = 1$ is used for fully crystalline state. Moreover, the wavelength-dependent dielectric permittivity function ($\varepsilon(\lambda)$) can be calculated based on the complex refractive index in the crystalline and amorphous state as $\varepsilon_a = n_a^2$ and $\varepsilon_c = n_c^2$.

Leveraging (1), the real and the imaginary part of the effective refractive index—which determines the phase delay and absorption of light in a material—of the PCM in an intermediate (mixed) state can be estimated as:

$$n_{eff} = \sqrt{\frac{\sqrt{(\varepsilon_1 + \varepsilon_2)^2 + \varepsilon_1}}{2}}, k_{eff} = \sqrt{\frac{\sqrt{(\varepsilon_1 + \varepsilon_2)^2 - \varepsilon_1}}{2}}, \quad (2)$$

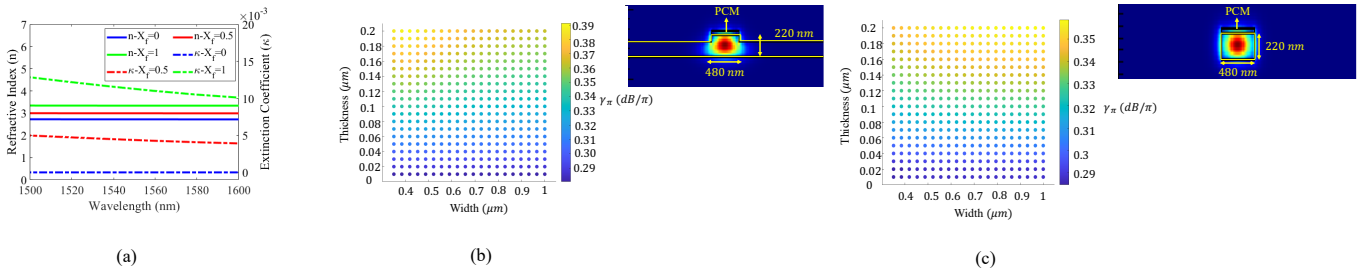


Fig. 2. (a) Optical refractive index (n) and extinction coefficient (κ) of Sb_2S_3 for three distinctive phase states of $X_f = 0, 0.5$, and 1. Optical loss (γ_π in dB/π) and optical mode profile (right-hand side) of (b) a ridge-waveguide-based and (c) a strip-waveguide-based phase modulator.

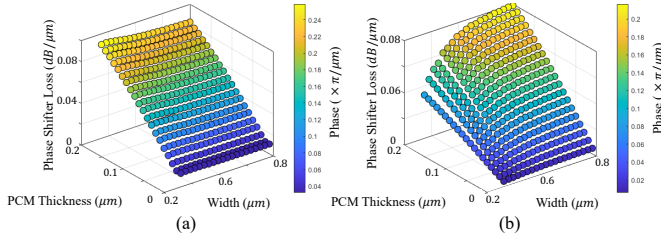


Fig. 3. Design-space exploration to analyze optical loss and phase shift under different design parameters: (a) strip waveguide and (b) ridge waveguide.

where ε_2 and ε_1 are, respectively, the real and imaginary part of $\varepsilon_{eff}(\lambda)$ in (1).

After analyzing the optical properties of the PCM in the intermediate states, finite-difference time-domain (FDTD) or finite-element modelling (FEM) simulations can be carried out to analyze the optical response of the PCM-based photonic device. The simplified flow for the simulation of PCM-based photonic devices is depicted in Fig. 1(a).

III. RESULTS AND DISCUSSIONS

Phase shifters are an integral part of integrated photonic modulators being used in photonic computing systems [6]. Therefore, as a case study, we present the design and simulation of a PCM-based phase modulator based on a strip and a ridge waveguide with a slab thickness of 150 nm [4], [6], as shown in Fig. 1(b). The PCM used for the phase shifter is Sb_2S_3 . Note that compared to GST or GSST, Sb_2S_3 has a lower extinction coefficient in different intermediate states, leading to a lower insertion loss for the resulting phase shifter [1], [7]. The optical refractive index and extinction coefficient of Sb_2S_3 for three distinctive phase states (i.e., $X_f = 0, 0.5$, and 1) are shown in Fig. 2(a). Phase shifter's π loss can be defined as $\gamma_\pi = \frac{\gamma_0 \pi}{\phi_0}$, where γ_0 is the insertion loss of the PCM-based phase shifter for 1 μm length and ϕ_0 is its corresponding achievable phase shift.

Assuming that the PCM's amorphous state ($X_f = 0$) corresponds to zero phase shift and crystalline state ($X_f = 1$) corresponds to π phase shift, a design-space exploration analysis is performed by sweeping the width and thickness of the PCM using Ansys Lumerical tools to capture the phase shifter's π loss under different design parameters and geometries. Note that in these simulations, the width of the waveguide is considered to be the same as the PCM's width. The phase shifter's π loss with different geometries for the

two designs using ridge and strip waveguides is depicted in Figs. 2(b) and 2(c), respectively. Observe that the effect of the PCM's thickness on the loss of the device is more critical than its width. Also, note that increasing the PCM's thickness leads to increased loss and response time (due to increased crystallization and amorphization time) of the phase shifter. The thickness of 40 nm and width of 480 nm are considered due to the low loss (i.e., 0.3 dB/π for both designs). We can see from Fig. 3 that the phase shift per length is 0.06 $\pi/\mu\text{m}$ for the strip and 0.03 $\pi/\mu\text{m}$ for the ridge design. This leads to a total length of $\approx 12 \mu\text{m}$ (with loss of 0.024 $\text{dB}/\mu\text{m}$) and $\approx 24 \mu\text{m}$ (with loss of 0.012 $\text{dB}/\mu\text{m}$) to induce a π phase shift at the operating wavelength of 1550 nm in, respectively, strip- and ridge-based phase shifters when the PCM is fully crystallized. Note that although the loss for the ridge design is lower than the strip design, the length of the ridge-based phase shifter is longer than the strip design. This leads to the same π -phase-shift optical loss for both designs.

The melting temperature for Sb_2S_3 is 823 K and the glass temperature is 473 K [8]. A microheater is designed based on Ti/TiN with $\rho = 60 \mu\Omega\cdot\text{cm}$ and sheet resistance of 5.5 Ω/sq to trigger the phase transition in the PCM (see Fig. 1(b)). The melting temperature of the heater material (Ti/TiN) is 1941 K, hence the heater material will not be melted when heating the PCM. The thickness of the heater is 110 nm with a width of 2 μm and length of 12 μm , placed 600 nm above the waveguide in order to reduce metallic absorption loss due to metal-light interaction [7]. Solving the transient unsteady-state heat-transfer equations (Ansys Lumerical HEAT was used) showed that an electrical pulse with a power of 20 mW and a duration of 24 μs can be used to reach the fully crystalline state. An electric pulse of 100 mW with a duration of 6.21 μs can be used to regain the amorphous state. Note that the phase transition of the Sb_2S_3 is assumed to be uniform over its volume. Further exploration of the application of the designed phase shifter in contemporary photonic devices can be done using the proposed multiphysics simulation approach.

REFERENCES

- [1] A. Shafiee *et al.*, *IEEE Access*, vol. 11, pp. 11 781–11 803, 2023.
- [2] C. Ríos *et al.*, *Nature photonics*, vol. 9, no. 11, pp. 725–732, 2015.
- [3] Y. Wang *et al.*, *npj Computational Materials*, vol. 7, no. 1, p. 183, 2021.
- [4] C. Ríos *et al.*, *PhotoniX*, vol. 3, no. 1, p. 26, 2022.
- [5] X. Li *et al.*, *Optica*, vol. 6, no. 1, pp. 1–6, 2019.
- [6] A. Mirza *et al.*, *IEEE TNANO*, vol. 21, pp. 763–771, 2022.
- [7] A. Shafiee *et al.*, *arXiv preprint arXiv:2303.15721*, 2023.
- [8] Y. Yang *et al.*, *Solar Energy*, vol. 217, pp. 25–28, 2021.